[CANCER RESEARCH 64, 547–553, January 15, 2004]

Radiation Improves the Distribution and Uptake of Liposomal Doxorubicin (Caelyx) in Human Osteosarcoma Xenografts

Catharina de L. Davies,[1] Lisa M. Lundstrøm,[1] Jomar Frengen,[2] Live Eikenes,[1] Øyvind S. Bruland,[3] Olav Kaalhus,[4] Mari H. B. Hjelstuen,[5] and Christian Brekken[5]

[1]Department of Physics, The Norwegian University of Science and Technology, Trondheim; [2]Department of Oncology, The University Hospital of Trondheim, Trondheim; Departments of [3]Radiotherapy and Oncology and [4]Biophysics, The Norwegian Radium Hospital, Oslo; and [5]Sintef Unimed MR Center, Trondheim, Norway

ABSTRACT

Liposomal drug delivery appears to improve the antitumor effect and reduce toxicity compared with the free drug. The therapeutic index may be improved further by combining cytotoxic drugs and radiotherapy. Successful therapy requires that the cytotoxic agents reach the tumor cells. Therefore, we studied tumor growth and the microdistribution of liposomal doxorubicin (Caelyx) with and without additional ionizing radiation in human osteosarcoma xenografts in athymic mice. Caelyx was injected i.v. 1 day before single or fractionated radiotherapy. Both chemoirradiation regimens induced significant tumor growth delays and worked synergistically. Confocal laser scanning microscopy showed that intact liposomes were located in close proximity to endothelial cells, and the distribution of released doxorubicin was heterogeneous. Before radiotherapy, hardly any doxorubicin was localized in the central parts of the tumor. Radiotherapy increased the tumor uptake of doxorubicin by a factor of two to four, with drug being redistributed farther from the vessels in the tumor periphery and located around vessels in the central parts of the tumor. Colocalization of doxorubicin and hypoxic cells showed no distribution of drug into hypoxic areas. Dynamic contrast-enhanced magnetic resonance imaging (MRI) 1 day before the injection of Caelyx and 2 days after treatment start showed that the combined treatment reduced the vascular volume and the vascular transfer rate of the MRI tracer. The results show that chemoirradiation with Caelyx induces synergistic treatment effects. Improved intratumoral drug uptake and distribution are responsible to some extent for the enhanced antitumor effect.

INTRODUCTION

Liposomal doxorubicin may enhance the antitumor effect, reduce toxicity, and improve pharmacokinetics compared with free doxorubicin. The polyethylene glycol (pegylated) coating reduces the uptake by cells of the reticuloendothelial system and prolongs the circulation time to a median half-life of approximately 45 h in humans (1). This, combined with the ability of liposomes to extravasate through leaky tumor vessels (2, 3), contributes to selective localization of liposomal doxorubicin in tumor tissue (4, 5). In normal tissue, the intact liposomes are confined to the intravascular space because normal blood vessels are not fenestrated to the same degree as tumor vessels. Therefore, toxicity to normal tissue is reduced considerably, particularly the cardiotoxicity of doxorubicin (6). Although liposomal delivery improves the tumor uptake compared with free drug, the drug distribution within the tumor tissue is heterogeneous (7, 8). To date, few studies have focused on the microdistribution of liposomal doxorubicin (7, 8).

Conventional anthracyclines are efficient radiosensitizers, and concomitant chemotherapy and radiotherapy improve the treatment outcome in a range of solid tumors. However, the increase in toxicity to normal tissue induced by such combined treatment is a major concern because radiotherapy and cytotoxic chemotherapy often share normal tissue toxicity profiles. Combining radiotherapy with liposomal delivery of anthracyclines may reduce this problem. Furthermore, sustained tumor-selective drug release from circulating liposomes during radiotherapy may improve the therapeutic index.

Liposomal doxorubicin has been found to increase the effect of single-dose and fractionated radiotherapy in animal models (9). Promising results have been reported for patients with non-small cell lung cancer and head and neck cancer (10). However, little is known about the mechanism underlying the improved therapeutic outcome. It has been suggested that the increased intratumoral accumulation of the drug improves the therapeutic outcome (9, 11). Radiation also has been reported to increase the tumor uptake of other macromolecules such as monoclonal antibodies (12, 13).

On the basis of the above, we postulated that radiotherapy, combined with liposomal doxorubicin, would improve the tumor uptake and intratumoral distribution of liposomal doxorubicin, thereby enhancing the antitumor effect compared with the two treatments administered separately. To test this hypothesis, liposomal doxorubicin was injected 1 day before irradiating athymic mice bearing human osteosarcoma xenografts. This treatment schedule was chosen to ensure the presence of the drug during irradiation [in the circulation, in extracellular matrix (ECM), and intracellularly] and thus to obtain doxorubicin-induced radiosensitization (9). The growth of the osteosarcomas was measured; the tumor uptake and distribution of liposomal doxorubicin were studied using confocal laser scanning microscopy (CLSM); and tumor vascular function was assessed with dynamic contrast-enhanced magnetic resonance imaging (MRI). The success of radiotherapy depends on the microenvironment within a tumor, and radioresistant hypoxic cells present a well-known obstacle to success. The distributions of liposomal doxorubicin in osteosarcomas growing at two different sites, either ectopically (s.c.) or orthotopically (around and infiltrating the femur), were compared accordingly, and liposomal doxorubicin was localized relative to the hypoxic areas.

MATERIALS AND METHODS

Animal and Tumor Models. Xenografts were grown in 7–9-week-old athymic female BALB/c-*nu/nu* mice (Möllergård Breeding Center, Copenhagen, Denmark) in two different microenvironments. Orthotopic (o.t.) or s.c. tumors were established by injecting a 100-μl suspension of 2×10^6 human osteosarcoma cells from the cell line OHS either adjacent to the periosteum of the femurs or s.c. (14). The o.t. tumors grew around and infiltrated the bones. Growth kinetics and histology of the two tumor models have been reported previously (15). The tumor dimensions were measured with a digital caliper. Tumor width and length were measured for the s.c. tumors. For the o.t. tumors, the two widths (width a and width b) of the leg of a mouse without a tumor and of the leg with a surrounding tumor were measured. Volumes were estimated using the formula for the volume of a prolate ellipsoid [s.c.: $V = \pi/6 \times (\text{width})^2 \times \text{length}$; o.t.: $V = \pi/6 \times (\text{width a})^2 \times (\text{width b})$]. The volumes of the o.t. tumors were estimated by subtracting the volume of the leg without a tumor from the volume of the leg with a surrounding tumor. For each animal, the tumor volume was normalized to the volume at treatment start. Tumor sizes

Received 3/10/03; revised 11/10/03; accepted 11/12/03.

Grant support: Norwegian Cancer Society and the Research Council of Norway.

The costs of publication of this article were defrayed in part by the payment of page charges. This article must therefore be hereby marked *advertisement* in accordance with 18 U.S.C. Section 1734 solely to indicate this fact.

Notes: M. H. B. H. is currently at the Department of Hemato-Oncology, Central Hospital of Rogaland, Stavanger, Norway; C. B. is currently at the Department of Circulation and Medical Imaging, The Norwegian University of Science and Technology, Trondheim, Norway.

Requests for reprints: Catharina de L. Davies, Department of Physics, The Norwegian University of Science and Technology, 7491 Trondheim, Norway.

in the different treatment groups (1 day before treatment) ranged from 0.9 ± 0.3 to 1.7 ± 0.3 cm^3 (mean ± SE). The animals were kept under pathogen-free conditions and allowed food and water *ad libitum*.

Treatments. Liposomal doxorubicin with a diameter of approximately 96 nm (Caelyx; Schering Plough, Oslo, Norway) was injected into the tail vein using 200 μl PBS containing 8 mg/kg in growth delay and MRI studies and 16 mg/kg in CLSM studies. The mice were anesthetized with an s.c. injection of Hypnorm, Dormicum (Janssen Pharmaceutical, Beerse, Belgium, and Alpharma AS, Oslo, Norway, respectively), and sterile water (1:1:2) using 1 ml/kg body weight. Liposomal doxorubicin was either given alone or combined with ionizing photon radiation. Ionizing radiation was given either as a single dose of 8 Gy the following day or as fractionated doses of 3.6 Gy for 3 subsequent days. Photon energy of 6 MV and a dose rate of 3–3.5 Gy/min were delivered by a Philips SL-75 linear accelerator (Crawley, UK). The mice were immobilized in a Plexiglas cylinder during irradiation. To achieve a sharp penumbra and minimal dose to the intestine, an 8-cm-thick lead shielding was applied 5 cm above the tumor. The control mice were untreated.

The doses of Caelyx and radiation were determined based on a pilot study of tumor growth after treatment with 1, 5, or 25 mg/kg of Caelyx alone or in combination with single-dose radiation of 13 Gy. The selected dose of Caelyx induced no significant effect on tumor growth when injected alone, and a significant, although not curable, effect on tumor growth when given in combination with radiation. The doses were 8 mg/kg in tumor growth and MRI studies, and 16 mg/kg in CLSM analyses to obtain sufficient fluorescence signals. A dose of 13 Gy was found to be too high; therefore, 8 Gy was chosen. The dose level of the fractionated regimen was determined experimentally to give a growth delay similar to the single fraction regimen using 8 Gy. According to the linear-quadratic formalism, this corresponds to an α:β ratio of 9.0 Gy.

Caelyx in solution (0.04 mg/ml) was irradiated (8 Gy) to test whether radiation would disintegrate the liposomes. Liposomal and released doxorubicin was separated by dialysis overnight, and then the fluorescence spectra were measured. The fluorescence intensity of free doxorubicin was three times higher than that of Caelyx in the spectral interval 530–700 nm, and thereby the free drug could be identified.

CLSM and MRI were done at coincident time points 2 days after the initiation of treatment, *i.e.,* 2 days after Caelyx injection and 1 day after the single dose of radiation given the day after Caelyx administration. MRI was performed additionally 1 day before the start of treatment. CLSM also was done subsequent to fractionated radiotherapy, and images were recorded 6 h after the last fraction, *i.e.,* 3 days after liposomal injection. These time points were chosen to assess whether the tumor vasculature was affected sufficiently by the irradiation to cause changes in the macromolecular transport within the tumor. A pilot study also showed maximum intratumoral accumulation of Caelyx 2–3 days after i.v. injection.[6]

The mice used in the tumor growth and MRI studies were killed by cervical dislocation once the diameter of the femur surrounded by the tumor exceeded 2 cm. The mice used in the CLSM studies were killed at the time of imaging. The tumors for microscopy studies were excised, embedded in Tissue Tec OCT Compound (Sakura, Zoeterwoude, the Netherlands), and frozen in liquid N_2, and 5-μm-thick frozen tumor sections were mounted on glass slides.

Fluorescence-Labeled Liposomes. Liposomes were labeled with a lipophilic tracer, the carbocyanine fluorophore 1,1′-dioctadecyl-3,3,3′,3′,-tetramethylindotricarbocyanine,4-chlorobenzenesulfonate salt (DiD; Molecular Probes, Eugene, OR). Five ml of 40 μg/ml DiD were incubated with 250 μl of 2 mg/ml Caelyx for 2 h at room temperature. Free DiD was separated from labeled liposomes using a Sephadex G-25 column (Amersham Biosciences, Piscataway, NJ). The liposome solution was concentrated to 5 mg/ml using microcollodion bags (Sartorius, Gottingen, Germany) connected to a pump. The concentration was measured by spectrophotometry and determined from the standard curve. Membrane-bound and unbound DiD could be distinguished by the fluorescence intensity because the fluorescence intensity of DiD in water is much less than in phospholipid membranes (16, 17).

Fluorescence-Labeled Blood Vessels. The sections were fixed in acetone for 10 min at room temperature and then incubated in goat serum to prevent nonspecific binding. The blood vessels on frozen sections were stained using rat antimouse CD31 antibody (clone MEC13.3; PharMingen, San Diego, CA) diluted to 16.7 μg/ml in PBS with 1% BSA. The antibody was visualized by incubating the sections with biotinylated goat antirat IgG (Vector Lab, Burlinghame, CA) for 30 min diluted to 10 μg/ml, followed by 30 min of incubation with streptavidin Alexa Fluor 633 or streptavidin Alexa Fluor 488 (Molecular Probes) diluted to 100 μg/ml. All of the incubations were at room temperature. The sections were rinsed in PBS between incubation.

Fluorescence-Labeled Hypoxic Cells. Hypoxic cells were labeled using pimonidazole, which binds covalently to hypoxic cells as a result of bioreduction by nitroreductases. Pimonidazole and the antiserum against the pimonidazole-protein adducts were supplied by Professor J.A. Raleigh (18). Thirty mg/kg pimonidazole in 100 μl were injected i.p., and the mice were killed 4 h later. Frozen sections were prepared as described earlier. Hypoxic cells were visualized by incubating the sections with rabbit antiserum to pimonidazole-protein adducts (diluted 1:1000) for 30 min at room temperature, rinsing them with PBS, and incubating them with goat antirabbit IgG conjugated to Alexa Fluor 488 (20 μg/ml; Molecular Probes) at room temperature for 30 min.

CLSM. Released doxorubicin, liposomes, and blood vessels were localized on frozen tumor sections using a CLSM (LSM510; Zeiss, Jena, Germany). Colocalization of doxorubicin, intact liposomes, and blood vessels was examined using a 20/0.3× objective. The intracellular location of doxorubicin was studied using a 63/1.3× water objective. A 488-nm argon laser line and 633-nm HeNe laser line were used to excite doxorubicin- and DiD-labeled liposomes, respectively. Detection of any spectral overlap was avoided by the multitrack function. The doxorubicin encapsulated in liposomes had a concentration that quenched the fluorescence. Doxorubicin does not bind covalently to the cells and therefore was washed away during the vessel-labeling procedure. Therefore, colocalization of doxorubicin and blood vessels had to be assessed by sequential imaging. The doxorubicin distribution was recorded before labeling the vessels, and then the same section and position were imaged with stained vessels. The sections were imaged along a radial track from periphery to center. The start position of the track was marked; based on this mark and the vessel structures, the two images could be overlaid easily. The colocalization of doxorubicin and the hypoxic areas was done sequentially in the same manner. All of the images had a resolution of 512 × 512 pixels. Laser current and detector gain were chosen to minimize noise and to use all of the gray values.

The uptake of doxorubicin was quantified by measuring the average fluorescence intensity per image. The fluorescence intensity was measured along a horizontal and vertical radial track from the periphery through the center to the other periphery. Six to 16 images were recorded per section, depending on the position of the section within the tumor and the size of the tumor. This was done for 10 sections per tumor and 3 tumors per treatment group. The sections were 150–200 μm apart, and the first section was approximately 2 mm from the tumor periphery. Quantitative measurements require that the fluorescence be neither attenuated nor bleached. Because the sections were only 5 μm thick, attenuation was negligible. The bleaching of doxorubicin fluorescence was measured by scanning sections continuously for 2 min. No change was observed in the fluorescence intensity, demonstrating the absence of bleaching with the settings used.

MRI and Data Analysis. MRI was performed 1 day before and 2 days after treatment start using a Bruker Biospec Avance DBX-100 (Bruker Biospin AG, Ettlingen, Germany) at 2.35 T with a saddle coil (inner diameter, 4 cm). A catheter (B. Braun Melsungen AG, Melsungen, Germany) was inserted into a tail vein, and the anesthetized animal was placed prone on a cradle filled with circulating fluorocarbons at a temperature of 37–38°C. The femur with tumor and the tail were placed in the coil. The key parameters describing the T1-weighted dynamic contrast-enhanced spin-echo pulse sequence were field of view, 3.0 cm; image matrix, 64 × 64; slices, 3; slice thickness, 3 mm; number of averages, 2; echo time, 5 ms; repetition time, 80 ms; frames, 60; and total experiment time, 16 min. A short bolus of 0.1 mmol/kg gadopentetate dimeglumine (Omniscan, Amersham Health Inc., Oslo, Norway) was injected after four initial baseline scans. Precontrast T1-maps were obtained from a set of images with identical sequence geometry and five consecutive acquisitions with echo time of 8.8 ms and repetition times of 1000, 400, 200, 100, and 58 ms. The MRI voxel size used (469 × 469 × 3000 μm^3) was too large to resolve the three main intratumoral fluid compartments spatially: the intravascular space, the ECM, and the intracellular space.

In the tracer kinetic model applied, each MRI voxel was modeled as consisting of two compartments: a plasma compartment and an extravascular compartment. Because the tracer (gadopentetate dimeglumine) does not enter

[6] Unpublished observations.

the cells, the extravascular compartment equals the extravascular extracellular space, *i.e.*, the ECM. The transport of tracer from the plasma compartments to the extravascular compartment can be characterized by the parameters: D_0 (mM) proportional to the blood plasma volume fraction and representing the maximum tracer concentration present in plasma during the experiment; D_1 (mM/min) proportional to the transfer constant of tracer from blood plasma to the extravascular compartment; and K_2 (min^{-1}) proportional to the transfer constant of tracer from the extravascular compartment to blood plasma and inversely proportional to the leakage space (19). The MRIs were analyzed offline on a personal computer using Interactive Data Language (IDL v5.4; Research Systems, Berkshire, United Kingdom). Dynamic contrast-enhanced images were analyzed on a whole tumor region of interest basis (>1000 pixels). Signal intensity was converted to Omniscan (Amersham Health Inc.) concentration based on precontrast T1 values. The kinetic constants D_0, D_1, and K_2 were estimated by curve fitting of the tracer concentration-*versus*-time curve according to Su *et al.* (19) {with a constant time-to-maximum plasma concentration [t_0(min)]}, and the arterial input function modified using published values for nude mice (20). The values reported are means of the average values in all of the three-image slices.

Apoptosis Detected by Flow Cytometry. To establish whether free doxorubicin and the single dose of radiation given, alone or in combination, were able to induce apoptosis and cell shrinkage, apoptosis and cell size were measured by flow cytometry for OHS cells growing as a monolayer. Flow cytometry has the advantage of measuring apoptosis and cell size simultaneously and then correlating these measurements per cell. To simulate the *in vivo* treatment, the cell line was incubated with 20 μM free doxorubicin alone for 48 h or for 24 h before and after ionizing radiation was given as a single dose of 8 Gy. Apoptosis was detected by the terminal deoxynucleotidyl transferase-mediated nick end labeling assay. Briefly, the cells were detached from the cell culture flasks using trypsin and fixed in 4% paraformaldehyde and permeabilized in 0.1% Triton. DNA strand breaks were detected by incubating the cells for 30 min at 37°C with a 35-μl solution containing biotin-dUTP and terminal deoxynucleotidyl transferase (Roche Diagnostics, Mannheim, Germany). After washing, the cells were labeled with 50 μl streptavidin-FITC diluted 1:50 (Dako, Glostrup, Denmark), washed, and DNA stained with 500 μl Hoechst 33258 (2 μg/ml; Molecular Probes). Apoptotic cells, DNA, and forward angle light scatter signal reflecting cell size were detected using a BD-LSR flow cytometer (Becton Dickinson, San Jose, CA) equipped with a 488-nm argon laser line and an UV laser. Untreated cells and cells labeled with streptavidin-FITC only had identical fluorescence histograms, and treated cells with FITC-fluorescence intensity higher than for these controls were detected as apoptotic cells.

Statistical Analysis. To evaluate synergism and additivity, the treatment effects were quantified using the difference in log tumor volume between the control and the treatment group (Caelyx, CX; radiation, RT; and combined treatment, RTCX in equations below). Individual pretreatment tumor variations were eliminated using log volume regression and normalizing the tumor volumes at treatment start to a common regression value. Thus, the subsequent variations in tumor volumes would be caused mainly by the individual responses to treatment. If normal regrowth occurs, one may assume an approximately exponential buildup of log tumor volume differences between the groups after treatment start. Data were taken from the first 15 days after treatment start, when the buildup of log tumor volume differences was approximately linear. These differences are considered statistically significant if the slope k of the built-up linear regression curve deviates significantly from zero at the $P = 0.05$ level. Chemotherapy and radiation were assumed to act by separate mechanisms, defined as Mode I by Steel and Peckham (21). Additivity predicts that the outcome of the combined regimen, relative to the control, should be equal to the sum of the effect of these two modalities (*i.e.*, $k_{CX} + k_{RT}$). If significantly larger, we conclude that the two modalities are acting synergistically. The synergy parameter, S, is defined as the ratio between this excess effect and the purely additive effect, $S_{RTCX} = [k_{RTCX} - (k_{CX} + k_{RT})]/(k_{CX} + k_{RT})$.

Statistical analyses of doxorubicin fluorescence intensity data at each time point, as well as number of apoptotic cells, were performed using one-way ANOVA. The number of images with fluorescence intensity of 0–10 pixel values was analyzed using a 5 × 3 contingency table and χ^2 test. The contingency table contained numbers of images with intensity values of 0 to 5 for the three groups: Caelyx alone and combined with single-dose or fractionated radiation. Statistical analysis of the MRI parameters was done using Student's t test. All of the statistical analyses were performed using the significance criterion of $P = 0.05$.

RESULTS

Tumor Growth Delay. The Caelyx dose (8 mg/kg) was chosen to give an almost negligible effect on tumor growth compared with the control. This is verified easily from Fig. 1 and the statistical analysis (log tumor volume difference slope ± SE $k_{CX} = 0.005 \pm 0.003\ d^{-1}$ in the interval 0–15 days). Treatment with radiation alone, either as a single dose of 8 Gy the following day or as fractionated radiation of 3.6 Gy for the 3 subsequent days, had considerable effects compared with the control (log tumor volume difference slope ± SE $k_{RT} = 0.05 \pm 0.005\ d^{-1}$ and $k_{fRT} = 0.04 \pm 0.004\ d^{-1}$, respectively; $P < 0.01$). When Caelyx and radiation were combined, the growth delay increased significantly, giving a slope of $k_{RTCX} = 0.09 \pm 0.005\ d^{-1}$ and $k_{fRTCX} = 0.08 \pm 0.006\ d^{-1}$ in the single-dose and fractionated cases. Compared with radiation alone, the additional effects are highly significant (log tumor volume difference slope ± SE $k_{RTCX\text{-}RT} = 0.04 \pm 0.005\ d^{-1}$ and $k_{fRTCX\text{-}fRT} = 0.04 \pm 0.004\ d^{-1}$, respectively; $P < 0.01$). Therefore, the statistical analysis indicates that there is a synergistic effect in both types of combined therapy: for single-dose radiotherapy and Caelyx treatment, the synergy parameter is $S_{RTCX} = 0.6 \pm 0.2$, and for fractionated radiation and Caelyx treatment, $S_{fRTCX} = 0.7 \pm 0.2$ (*i.e.*, a 60% and 70% increase compared with the purely additive effects). Consistent with this, the corresponding doubling times are on the order of 7–8 days for the control and Caelyx treatment groups, 13–16 days for the radiation alone groups, and 22–27 days for the combination therapy groups.

Distribution of Liposomes and Released Doxorubicin in Osteosarcomas. Intact liposomes were located in close proximity to endothelial cells or within blood vessels (Fig. 2). Few intact liposomes were observed, indicating an efficient degradation of the liposomes and release of the drug. This degradation is the result of enzymatic disintegration in the interstitium because radiation was found not to disintegrate Caelyx. Irradiation (8 Gy) of Caelyx in solution did not affect the fluorescence spectra, and after dialysis of Caelyx, no doxorubicin was detected in the solution outside the dialysis bag.

Doxorubicin released from the liposomes penetrated farther from the vessels. In the periphery of the tumor, the drug was located up to 450 μm from the rim of the tumor. By imaging the tumor sections

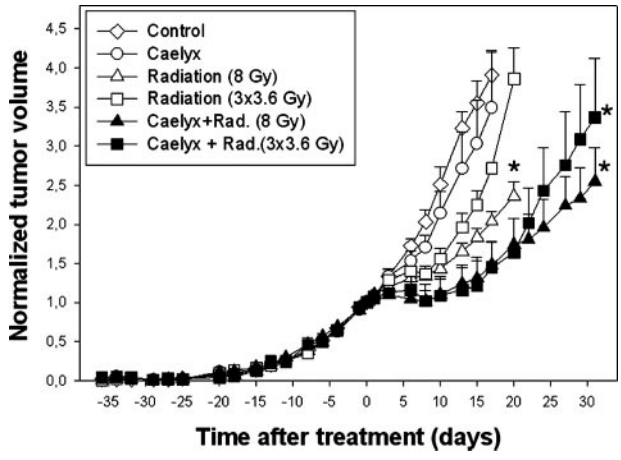

Fig. 1. Tumor growth normalized to tumor volume at treatment start. The tumors were untreated (◇; $n = 8$) or given Caelyx alone, 8 mg/kg (○; $n = 6$), single-dose radiation, 8 Gy (△; $n = 8$), fractionated radiation, 3 × 3.6 Gy (□; $n = 8$), Caelyx in combination with single-dose radiation (▲; $n = 8$), or combined with fractionated radiation (■; $n = 7$). Each symbol is the mean of n mice; *bars*, ± SE. *Growth curves significantly different from untreated controls.

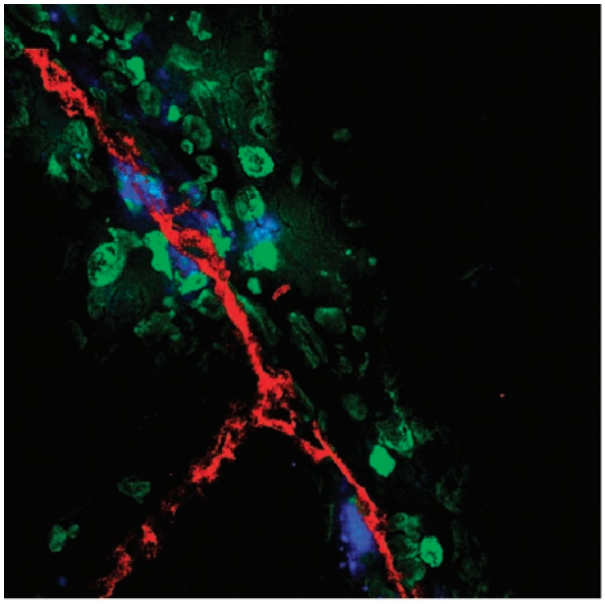

Fig. 2. Localization of intact 1,1′-dioctadecyl-3,3,3′,3′,-tetramethylindotricarbocyanine,4-chlorobenzenesulfonate salt (*DiD*) labeled liposomes (blue) and released doxorubicin (green) relative to capillaries (red).

along a radial track from the periphery to the center of the section, the distribution of doxorubicin in the periphery and central parts of the tumor was compared. In tumors treated with Caelyx only, hardly any doxorubicin fluorescence was detected in the central part of the tumor (Fig. 3, *A* and *C*). Radiation improved considerably the distribution of doxorubicin, although doxorubicin was distributed rather heterogeneously. Radiation allocated doxorubicin farther from the vessels in the periphery, and doxorubicin was located around vessels in the central part of the section where no doxorubicin was observed in tumors treated with Caelyx alone (Fig. 3, *B* and *D*).

Intracellular Location of Doxorubicin. Doxorubicin was located intracellularly. Hardly any fluorescence was seen in the ECM. The intracellular distribution of doxorubicin was heterogeneous, located in the nuclei and the cytoplasm. In the cytoplasm, doxorubicin fluorescence was either diffuse or granular, the latter indicating vesicular or lysosomal localization. Radiation did not change the intracellular distribution.[6]

Impact of the Microenvironment on Doxorubicin Distribution. The influence of the microenvironment on doxorubicin distribution was studied by comparing osteosarcomas growing o.t. around the femur and s.c. (Fig. 3). At both tumor sites, doxorubicin was distributed heterogeneously and located mainly in the periphery of the tumor. Radiation improved the distribution of doxorubicin in the same manner in both tumor models. However, somewhat less doxorubicin was seen in the s.c. tumors than in the o.t. ones.

Quantitative Measurements of Doxorubicin Uptake. To obtain more quantitative data on doxorubicin distribution and uptake, the doxorubicin fluorescence intensity was quantitated by estimating the average pixel intensity per image and by estimating the fluorescence pixel area per image. Both measurements gave similar results. The measurements were made along two perpendicular tracks radial on 10 sections per tumor in three tumors. The uptake of doxorubicin in the periphery was 5 to 10 times higher than in the other parts of the tumors given liposomal doxorubicin alone, and 3 to 8 times higher in the periphery of the tumors given liposomal doxorubicin combined with radiation (Fig. 4). Radiation increased the uptake of liposomal doxorubicin in the central parts of the tumor approximately two to four times after single 8-Gy dose and one to three times after 3×3.6 Gy (Fig. 4).

The ratio between doxorubicin fluorescence intensity in the periphery and central parts of the tumor and the effect of single-dose radiation was approximately the same in the tumors growing o.t. and s.c. (Fig. 4). However, the o.t. tumors had approximately twice as high doxorubicin fluorescence intensity in the periphery as the s.c. tumors, both those treated with Caelyx alone and in combination with a single

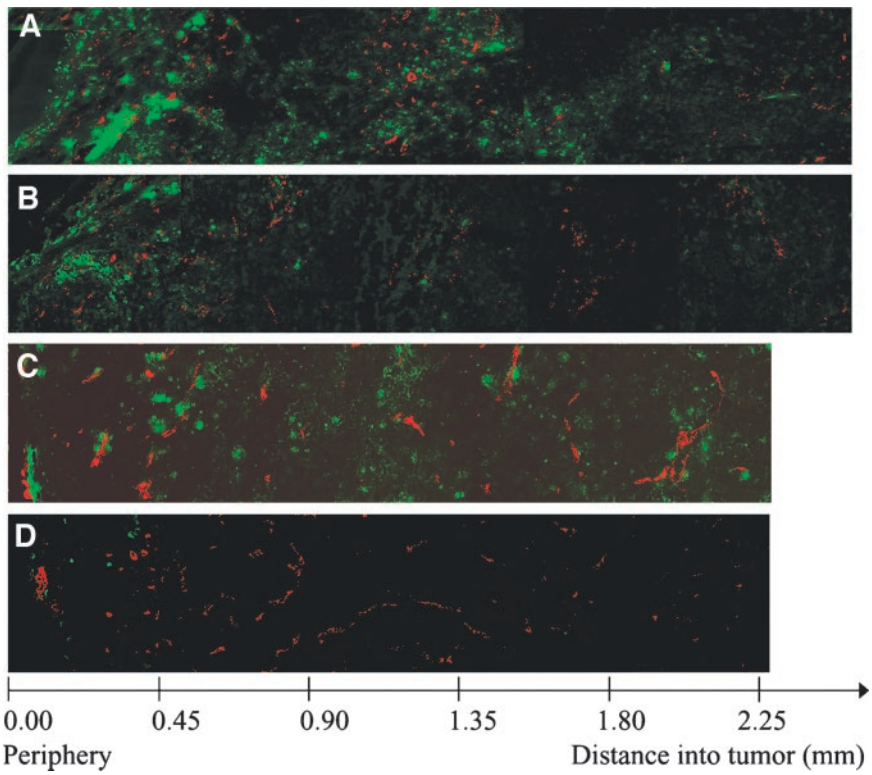

Fig. 3. Distribution of liposomal doxorubicin in orthotopic (*A* and *B*) and s.c. (*C* and *D*) tumors treated with Caelyx alone (16 mg/kg; *B* and *D*) or Caelyx combined with single-dose radiation (8 Gy; *A* and *C*). Representative images 2 days after treatment start show doxorubicin (green) relative to capillaries (red) from the rim to the center of the tumor sections.

dose of radiation. In the central part of the o.t. tumors treated with Caelyx alone, the doxorubicin fluorescence intensity was up to three to six times higher than in the s.c. tumors, whereas little difference was seen in doxorubicin intensity when combined with radiation (Fig. 4).

The improved distribution of doxorubicin after radiotherapy also was demonstrated by plotting the number of images as a function of fluorescence intensity. Tumors treated with Caelyx and radiation had a higher number of images with detectable fluorescence than tumors treated with Caelyx only (Fig. 5). This shows that radiation redistributed doxorubicin to more areas of the tumors.

Doxorubicin Relative to Hypoxic Cells. The improved distribution of doxorubicin after radiotherapy did not allocate doxorubicin to hypoxic areas. Although radiation made doxorubicin penetrate farther from the blood vessels, it was distributed heterogeneously and not able to penetrate in hypoxic areas.[6]

Tumor Microvascular Function. All of the three MRI-derived parameters relating to tumor microvascular function (D_0, D_1, and K_2) were reduced 2 days after treatment start when Caelyx was combined with 8 Gy of radiation. No significant changes in the three MRI-derived parameters were found in the control group or in the group treated with Caelyx alone (Fig. 6).

Induction of Apoptotic Cells. The treatment combining free doxorubicin (20 μM) and a single dose of radiation (8 Gy) increased significantly the number of apoptotic cells compared with radiotherapy alone. The flow cytometric measurements were done 2 days after the start of treatment. The dose of doxorubicin induced a rather large number of apoptotic cells, and no significant difference was found between doxorubicin alone or combined with radiation (Fig. 7).

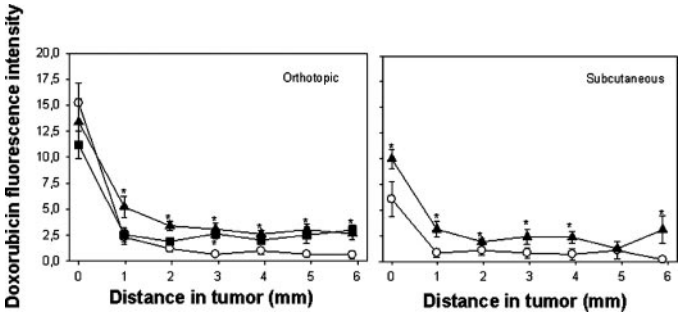

Fig. 4. Doxorubicin fluorescence intensity profile in orthotopic (*left*) and s.c. (*right*) tumors treated with Caelyx alone (16 mg/kg; ○) or combined with single-dose radiation (8 Gy; ▲) or fractionated radiation (3 × 3.6 Gy; ■). Pixel values are plotted as a function of distance from the rim to the center of the tumor section 2 or 3 days after Caelyx injection combined with single-dose or fractionated radiotherapy, respectively. Each symbol is the mean of 12–32 images per section and 10 sections per tumor in three tumors; *bars*, ±SE. *Fluorescence intensity significantly different from Caelyx alone.

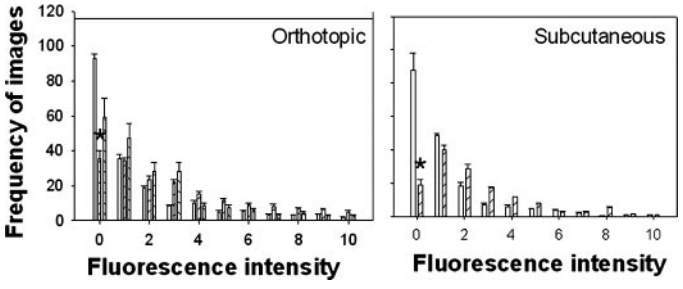

Fig. 5. Frequency of images with fluorescence intensity of 0–10 pixel values for orthotopic (*left*) and s.c. (*right*) tumors treated with Caelyx alone (16 mg/kg; □) or combined with single-dose radiation (8 Gy; ▨) or fractionated radiation (3 × 3.6 Gy; ▧). Each value is the mean of 12–32 images per section and 10 sections per tumor in three tumors 2 or 3 days after Caelyx injection combined with single-dose or fractionated radiotherapy, respectively; *bars*, ±SE. *Data significantly different from Caelyx alone.

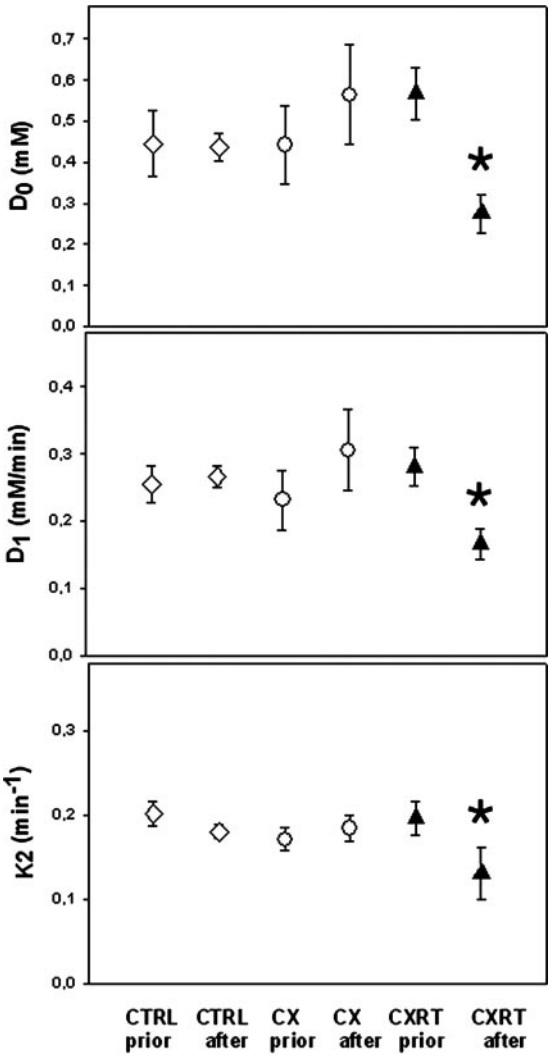

Fig. 6. Magnetic resonance imaging-derived estimates of contrast agent tracer kinetic parameters: D_0, proportional to the blood plasma volume fraction; D_1, proportional to the transfer constant from blood to interstitium; and K_2, proportional to transfer constant from interstitium to blood and inversely proportional to leakage space. No treatment (*CTRL*; ◇), 8 mg/kg Caelyx (*CX*; ○), and 8 mg/kg Caelyx + 8 Gy radiation (*CXRT*; ▲). Values are means of four to seven animals; *bars*, ±SE. *Prior* and *after* refer to the same animal group 1 day before and 2 days subsequent to treatment start, respectively. *Data significantly different from untreated controls.

DISCUSSION

Concomitant Radiotherapy and Liposomal Doxorubicin Delayed Tumor Growth. Liposomal delivery of doxorubicin, administered in combination with single-dose or fractionated radiotherapy, delayed the growth of human osteosarcoma xenografts. To obtain information about the mechanisms underlying the interactions, statistical analysis was performed on the tumor growth data. On the basis of the doses used, it was found that Caelyx had an almost negligible effect on tumor growth. However, combined with radiation, the effect was significantly larger than the purely additive effect (*i.e.*, the sum of the chemotherapy and radiotherapy effect considered separately). Thus, doxorubicin and radiation interacted positively, and the synergistic effect was found to be approximately the same in the two radiotherapy regimens. Direct inactivation of radioresistant hypoxic cells by doxorubicin probably was not a contributing factor to the delayed tumor growth because doxorubicin was not redistributed to hypoxic areas after radiation.

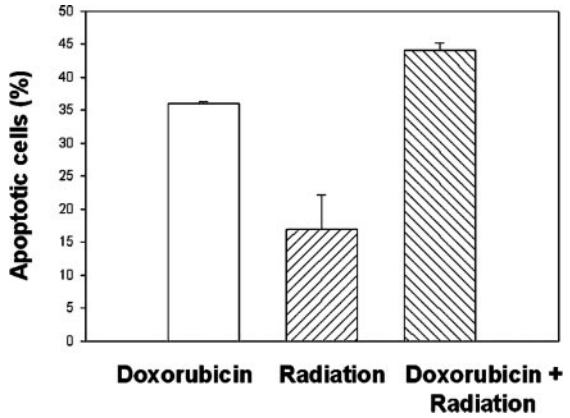

Fig. 7. Percentage of apoptotic cells growing in monolayer induced by doxorubicin (20 μM) and radiation (8 Gy) alone or in combination. Each value is the mean of three measurements; *bars*, ±SE.

Distribution and Uptake of Liposomal Doxorubicin Were Improved by Radiation. Successful delivery of doxorubicin to the tumor cells requires that circulating liposomes extravasate and release doxorubicin that has to penetrate through the ECM. Therefore, to investigate further the synergistic mechanism of the action between Caelyx and ionizing radiation, CLSM and MR images of treated tumor tissue were analyzed at coincident time points in the treatment schedule. The CLSM images demonstrated that doxorubicin released from the liposomes was located mainly in the tumor periphery before and after radiotherapy. After radiotherapy, doxorubicin also was localized around vessels in the central parts of the tumor, demonstrating that the liposomes had been able to extravasate into the interstitium where they were disintegrated chemically, probably because of enzymes, low pH, and oxidative agents in the interstitium (22). Radiation was found not to disintegrate the liposomes. The uptake of doxorubicin in the central parts of the tumor increased two to four times after a single dose of radiation and one to three times after fractionated radiation. This increased accumulation of doxorubicin may be a factor of the schedule of liposomal doxorubicin administration and irradiation. In a study by Harrington *et al.* (23), radiation was given at various times before i.v. injection of radiolabeled Caelyx, and no increase was found in the tumor uptake of Caelyx. However, consistent with our study, they found a significant increase in the growth delay of xenografts treated with radiation administered 16 h after an i.v. injection of Caelyx (9).

The contrast-enhanced MR images showed that a single fraction of radiation combined with Caelyx reduced the vascular transfer rate and the vascular volume. These vascular parameters were obtained using a tracer kinetic model. The transfer rate from blood to interstitium reflects the vascular permeability for the low molecular contrast agents, suggesting that radiation also reduces the transfer rate of high molecular weight Caelyx. Therefore, the improved distribution of liposomal doxorubicin is not caused by increased vascular transfer rate and volume. The observed reduction in vascular transfer rate is not consistent with other findings indicating that radiation increases vascular permeability (24, 25), probably because of an increase in the level of vascular endothelial growth factor (26). This discrepancy may have several explanations. For example, the radiation-induced vascular effects are dynamic and time dependent, and the results depend on the doses and time of measurement. The observed reduction in the vascular transfer rate may be caused by a decrease in the vascular surface area for exchange caused by a total collapse of vessels or a reduction in vessel radius, rather than by a reduction in the vascular permeability of functional vessels. The observed decrease in vascular volume, which is consistent with other studies (25, 27, 28), supports this. The discrepancy also may be the result of different effects on the vasculature by radiation combined with Caelyx than by radiation given alone, because CLSM images showed doxorubicin located inside the endothelial cells.

The transvascular liposomal flux is governed by a transvascular pressure gradient and/or concentration gradient. An increase in the pressure gradient could arise from a radiation-induced increase in microvascular pressure and/or a decrease in interstitial fluid pressure (IFP) (29). A collapse of vessels and/or a decrease in vessel radius demonstrated by the decrease in vascular volume potentially could increase vascular resistance, thereby increasing microvascular pressure. The importance of a transvascular pressure gradient for the delivery of liposomal doxorubicin was demonstrated by the intense doxorubicin fluorescence in the tumor periphery in nonirradiated and irradiated tumors alike. For nonirradiated tumors, doxorubicin fluorescence was detected from the rim and up to 450 μm into the tumor. This fluorescent region of the tumor correlates spatially with the tumor region where a decrease in IFP was observed (30). In our OHS xenograft model growing s.c., we also have demonstrated a high IFP in the interior of the tumor and a steep pressure gradient in the periphery.[7] Another explanation for the increased doxorubicin uptake in the tumor periphery could be the higher vascular density in this area compared with in central parts of the tumor (31). Liposomal accumulation has been reported to correlate with vascular density (10).

Inside the interstitium, the main transport mechanism of liposomes and released doxorubicin probably is diffusion because of the high IFP in the central parts of the tumor (15). However, the images showed that liposomes were not able to diffuse away from the blood vessels and that doxorubicin was able to diffuse only a short distance. The diffusion coefficient decreases with increasing molecular weight, thereby limiting the diffusion of intact liposomes to a much greater extent than the released doxorubicin (32). Inefficient diffusion is caused by the tortuous nature of the pathways and steric exclusion by the ECM network and cells, and would have limited impact on the small molecule doxorubicin. Efficient cellular uptake of doxorubicin, impeding further interstitial penetration of doxorubicin, is another factor that contributes to the heterogeneous distribution of doxorubicin. The improved distribution of doxorubicin after radiotherapy may be ascribable to induced apoptosis and cell shrinkage, which destroy integrin-based ECM anchorages and destabilize the ECM structure, which may increase diffusion and convection (33).

Other treatments, such as hyperthermia and enzymatic degradation of ECM, increased the tumor uptake of liposomal doxorubicin. The uptake of liposomal, but not free, doxorubicin was improved in rodent tumors after hyperthermia (34, 35). Intratumoral injection of hyaluronidase before Caelyx administration in the OHS xenografts induced similar improvements in tumor distribution and uptake as found in the present study (36). Thus, liposomal delivery of doxorubicin seems to have advantages compared with free doxorubicin when administered in combination with various treatments.

Impact of the Microenvironment on the Distribution of Liposomal Doxorubicin. Osteosarcoma xenografts growing o.t. around the femur had a higher uptake of doxorubicin than was measured in s.c. xenografts. In both tumor models, doxorubicin was located mainly in the periphery of the tumor. The enhanced doxorubicin uptake in o.t. tumors may be caused by differences in IFP, ECM content and structure, and vascularization observed in tumors growing at the two sites. Tumors growing o.t. are found to have a higher IFP and vascular density than s.c. growing tumors (37). The CLSM images in the present study confirm that o.t. tumors have a higher vascular density,

[7] L. Eikenes, Ø. S. Bruland, C. Brekken, and C. de L. Davies. Collagenase increases the transcapillary pressure gradient and improves the uptake and distribution of monoclonal antibodies in human osteosarcoma xenografts, submitted for publication.

but the radii of the vessels are smaller than in s.c. tumors. Radiation improved the distribution of doxorubicin in the same way in both tumor models because doxorubicin was localized farther into the tumor and primarily around blood vessels in both tumor models. Thus, the effect of concomitant radiotherapy and doxorubicin on ECM and vasculature appeared to be independent of the site of tumor growth.

Clinical Implications. Doxorubicin is one of the most commonly used agents for the management of osteosarcoma (38, 39). New treatment strategies are needed to further improve the outcome, particularly for osteosarcoma patients with primary tumors localized to the axial skeleton (38, 40, 41). Concomitant adjuvant chemoirradiation using doxorubicin does not seem feasible because of the severe toxicity resulting from the elevated production of toxic free radicals (42). Liposomal delivery of cytotoxic agents is one promising approach because it increases the tumor uptake of the drug and reduces toxicity compared with the free drug (43). The therapeutic response is increased further using concomitant chemoirradiation based on liposomal delivery of doxorubicin (10). The present work demonstrates that the synergy achieved can be explained in part by improved intratumoral drug uptake and distribution.

ACKNOWLEDGMENTS

We thank Tina Bugge Pedersen and Emil Veliyulin for their technical assistance. We also thank Kristin Bringedal, Department of Pathology, University Hospital of Trondheim, for preparing frozen tissue sections.

REFERENCES

1. Gabizon, A., Catane, R., Uziely, B., Kaufman, B., Safra, T., Cohen, R., Martin, F., Huang, A., and Barenholz, Y. Prolonged circulation time and enhanced accumulation in malignant exudates of doxorubicin encapsulated in polyethylene-glycol coated liposomes. Cancer Res., *54:* 987–992, 1994.
2. Wu, N. Z., Da, D., Rudoll, T. L., Needham, D., Whorton, R., and Dewhirst, M. W. Increased microvascular permeability contributes to preferential accumulation of Stealth liposomes in tumor tissue. Cancer Res., *53:* 3765–3770, 1993.
3. Yuan, F., Leunig, M., Huang, S. K., Berk, D. A., Papahadjopoulos, D., and Jain, R. K. Microvascular permeability and interstitial penetration of sterically stabilized (Stealth) liposomes in a human tumor xenograft. Cancer Res., *54:* 3352–3356, 1994.
4. Gabizon, A., and Martin, F. Polyethylene glycol-coated (pegylated) liposomal doxorubicin. Drugs, *54* (Suppl. 4)*:* 15–21, 1997.
5. Symon, Z., Peyser, A., Tzemach, D., Lyass, O., Sucher, E., Shezen, E., and Gabizon, A. Selective delivery of doxorubicin to patients with breast carcinoma metastases by Stealth liposomes. Cancer (Phila.), *86:* 72–78, 1999.
6. Harris, L., Batist, G., Belt, R., Rovira, D., Navari, R., Azarina, N., Welles, L., and Winer, E. Liposome-encapsulated doxorubicin compared with conventional doxorubicin in a randomized multicenter trial as first-line therapy of metastatic breast carcinoma. Cancer (Phila.), *94:* 25–36, 2002.
7. Huang, S. K., Lee, K-D., Hong, K., Friend, D. S., and Papahadjopoulos, D. Microscopic localization of sterically stabilized liposomes in colon carcinoma-bearing mice. Cancer Res., *52:* 5135–5143, 1992.
8. Vaage, J., Donovan, D., Uster, P., and Working, P. Tumor uptake of doxorubicin in polyethylene glycol-coated liposomes and therapeutic effect against a xenografted human pancreatic carcinoma. Br. J. Cancer, *75:* 482–486, 1997.
9. Harrington, K. J., Rowlinson-Busza, G., Syrigos, K. N., Vile, R. G., Uster, P. S., Peters, M., and Stewart, J. S. W. Pegylated liposome-encapsulated doxorubicin and cisplatin enhance the effect of radiotherapy in a tumor xenograft model. Clin. Cancer Res., *6:* 4939–4949, 2000.
10. Koukourakis, M. I., Koukouraki, S., Giatromanolaki, A., Archimandritis, S. C., Skarlatos, J., Beroukas, K., Bizakis, J. G., Retalis, G., Karavitsas, N., and Helidonis, E. S. Liposomal doxorubicin and conventionally fractionated radiotherapy in the treatment of locally advanced non-small-cell lung cancer and head and neck cancer. J. Clin. Oncol., *17:* 3512–3521, 1999.
11. Koukourakis, M. I., Koukourakis, S., Giatromanolaki, A., Kakolyris, S., Georgoulias, V., Velidaki, A., Archimandritis, S., and Karkavitsas, N. N. High intratumoral accumulation of Stealth liposomal doxorubicin in sarcomas. Rationale for combination with radiotherapy. Acta Oncol., *39:* 207–211, 2000.
12. Kalofonos, H., Rowlinson, G., and Epenetos, A. A. Enhancement of monoclonal antibody uptake in human colon tumor xenografts following irradiation. Cancer Res., *50:* 159–163, 1990.
13. Stickney, D. R., Gridley, D. S., Kirk, G. A., and Slater, J. M. Enhancement of monoclonal antibody binding to melanoma with single dose radiation or hyperthermia. NCI Monogr., *3:* 47–52, 1987.
14. Fodstad, Ø., Brøgger, A., Bruland, Ø., Solheim, Ø. P., Nesland, J. M., and Pihl, A. Characteristics of a cell line established from a patient with multiple osteosarcoma, appearing 13 years after treatment for bilateral retinoblastoma. Int. J. Cancer, *38:* 33–40, 1986.
15. Brekken, C., Bruland, Ø. S., and Davies, C. de. L. Interstitial fluid pressure in human osteosarcoma xenografts: significance of implantation site and the response to intratumoral injection of hyaluronidase. Anticancer Res., *20:* 3503–3512, 2000.
16. Haugland R. P. Handbook of Fluorescent Probes and Research Products, p. 573. Eugene, OR: Molecular Probes, 2002.
17. Honig, M. G., and Hume, R. I. Fluorescent carbocyanine dyes allow living neurons of identified origin to be studied in long-term cultures. J. Cell Biol., *103:* 171–187, 1986.
18. Raleigh, J. A., Chou, S-C., Arteel, G. E., and Horsman, M. R. Comparisons among pimonidazole binding, oxygen electrode measurements, and radiation response in C3H mouse tumors. Radiat. Res., *151:* 580–589, 1999.
19. Su, M-Y., Jao, J-C., and Nalcioglu, O. Measurement of vascular volume fraction and blood-tissue permeability constants with a pharmacokinetic model: studies in rat muscle tumors with dynamic Gd-DTPA enhanced MRI. Magn. Reson. Med., *32:* 714–724, 1994.
20. Furman-Haran, E., Grobgeld, D., and Degani, H. Dynamic contrast-enhanced imaging and analysis at high spatial resolution of MCF7 human breast tumors. J. Magn. Reson., *128:* 161–171, 1997.
21. Steel, G. G., and Peckman, M. J. Exploitable mechanisms in combined radiotherapy-chemotherapy: the concept of additivity. Int. J. Radiat. Oncol. Biol. Phys., *5:* 85–91, 1979.
22. Martin, F. J. Pegylated liposomal doxorubicin: scientific rationale and preclinical pharmacology. Oncology, *11* (Suppl.)*:* 11–20, 1997.
23. Harrington, K. J., Rowlinson-Busza, G., Uster, P. S., Vile, R. G., Peters, A. M., and Stewart, J. S. W. Single-fraction irradiation has no effect on uptake of radiolabeled pegylated liposomes in a tumor xenograft model. Int. J. Radiat. Oncol. Biol. Phys., *49:* 1141–1148, 2001.
24. Cohen, F. M., Kuwatsuru, R., Shames, D. M., Neuder, M., Mann, J. S., Vexler, V., Rosenau, W., and Brasch, R. C. Contrast-enhanced magnetic resonance imaging estimation of altered capillary permeability in experimental mammary carcinomas after X-irradiation. Invest. Radiol., *29:* 970–977, 1994.
25. Song, C. W., and Levitt, S. H. Effect of X irradiation on vascularity of normal tissues and experimental tumors. Radiology, *94:* 445–447, 1970.
26. Park, J-S., Qiao, L., Su, Z-Z., Hinman, D., Willoughby, K., McKinstry, R., Yacoub, A., Duigou, G. J., Young, C. S. H., Grant, S., Hagan, M. P., Ellis, E., Fisher, P. B., and Dent, P. Ionizing radiation modulates vascular endothelial factor (VEGF) expression through multiple mitogen activated protein kinase dependent pathways. Oncogene, *20:* 3266–3280, 2001.
27. Solesvik, O., Rofstad, E. K., and Brustad, T. Vascular changes in a human malignant melanoma xenograft following single-dose irradiation. Radiat. Res., *98:* 115–128, 1984.
28. Edwards, E., Geng, L., Tan, J., Onishko, H., Donnelly, E., and Hallahan, D. E. Phosphatidylinositol 3-kinase/Akt signaling in the response of vascular endothelium to ionizing radiation. Cancer Res., *62:* 4671–4677, 2002.
29. Znati, C. A., Rosenstein, M., Boucher, Y., Epperly, M. W., Bloomer, W. D., and Jain, R. K. Effect of radiation on interstitial fluid pressure and oxygenation in a human tumor xenograft. Cancer Res., *56:* 964–968, 1996.
30. Boucher, Y., Baxter, L. T., and Jain, R. K. Interstitial pressure gradients in tissue-isolated and subcutaneous tumors: implications for therapy. Cancer Res., *50:* 4478–4484, 1990.
31. Graff, B. A., Kvinnsland, Y., Skretting, A., and Rofstad, E. K. Intratumour heterogeneity in the uptake of macromolecular therapeutic agents in human melanoma xenografts. Br. J. Cancer, *88:* 291–297, 2003.
32. Pluen, A., Netti, P. A., Jain, R. K., and Berk, D. A. Diffusion of macromolecules in agarose gels: comparison of linear and globular configurations. Biophys. J., *77:* 542–552, 1999.
33. Barcellos-Hoff, M. H., and Ravani, S. A. Irradiated mammary gland stroma promotes the expression of tumorigenic potential by unirradiated epithelial cells. Cancer Res., *60:* 1254–1260, 2000.
34. Ning, S., Macleod, K., Abra, R. M., Huang, A. H., and Hahn, G. M. Hyperthermia induces doxorubicin release from long-circulating liposomes and enhances their anti-tumor efficacy. Int. J. Radiat. Oncol. Biol. Phys., *29:* 827–834, 1994.
35. Monsky, W. L., Kruskal, J. B., Lukyanov, A. N., Girnun, G. D., Ahmen, M., Gazelle, G. S., Huertas, J. C., Stuart, K. E., Torchilin, V. P., and Goldberg, S. N. Radiofrequency ablation increases intratumoral liposomal doxorubicin accumulation in a rat breast tumor model. Radiology, *224:* 823–829, 2002.
36. Davies, C. de L., Bruland, Ø. S., and Tari, M. R. Hyaluronidase improves the distribution of liposomal doxorubicin in human osteosarcoma xenografts. Int. J. Cancer, *13* (Suppl.)*:* 425, 2002.
37. Davies, C. de L., Engeseter, B., Haug, I., Ormeberg, I. W., Halgunset, J., and Brekken, C. Uptake of IgG in osteosarcoma correlates inversely with interstitial fluid pressure, but not with interstitial constituents. Br. J. Cancer, *85:* 1986–1977, 2001.
38. Bruland, Ø. S., and Pihl, A. On the current management of osteosarcoma. A critical evaluation and a proposal for a modified treatment strategy. Eur. J. Cancer, *33:* 1725–1731, 1997.
39. Ferguson, W. S., and Goorin, A. M. Current treatments of osteosarcoma. Cancer Invest., *19:* 292–315, 2001.
40. Sæter, G., Bruland, Ø. S., Follerås, G., Boysen, M., and Høie, J. Extremity and non-extremity high-grade osteosarcoma—the Norwegian Radium Hospital experience during the modern chemotherapy era. Acta Oncol., *35:* 129–134, 1996.
41. Anderson, P. M., Wiseman, G. A., Dispenzeri, A., Arndt, C., Hartman, L. C., Smithson, W. A., Mullan, B. P., and Bruland, Ø. S. High dose 153-samarium ethylene diamine tetramethylene phosphonate: low toxicity of skeletal irradiation in patients with osteosarcoma and bone metastases. J. Clin. Oncol., *20:* 189–196, 2002.
42. Freyer, G., and Romestaing, P. Chemoradiation and breast cancer. *In:* F. Mornex, J. J. Mazeron, J. P. Droz, and M. Marty (eds.), Concomitant Chemoradiation: Current Status and Future, pp. 185–188. Paris: Elsevier, 2002.
43. Gabizon, A., Shmeeda, H., and Barenholz, Y. Pharmacokinetics of pegylated liposomal doxorubicin. Review of animal and human studies. Clin. Pharmacokinet., *42:* 419–436, 2003.